IOSR Journal of Engineering (IOSRJEN)
e-ISSN: 2250-3021, **p**-ISSN: 2278-8719
Vol. 3, Issue 6 (June. 2013), ||V3|| PP 12-16

Tensile Properties and Gamma Precipitates in Grain Boundaries of Nickel Alloys

Aezeden Mohamed
Faculty of Engineering and Applied Science, Memorial University, St. Johns, NL, Canada, A1B 3X5

Abstract : - The effects of alloying additions, Cr and Mo, on the tensile properties, plastic deformation behaviours, and fracture mechanisms of nickel alloys, including IN600, IN601, C22, were investigated through uniaxial tensile testing. Test specimens were annealed and air-cooled. From the resulting stress strain curve (SSC), it was found that alloy C22 exhibited higher strength and ductility than IN600 and IN601. Dimpled ductile intergranular fractures were obtained and it was determined that the Mo and Cr additions prevented premature brittle intergranular failure. It was also found that the microstructural characterizations of C22 showed higher amounts of slip bands within grains than IN600 and IN601. Higher plasticity and strength of the C22 alloy is indicated.

Keywords: *- C22; IN601; IN600; dimple; intergranular fracture; slip bands; tensile test.*

I. INTRODUCTION

Choosing the right materials and heat treatments are the primary key for success in obtaining excellent mechanical properties of metallic materials, including nickel-based chromium alloys, comprising mainly nickel, chromium, iron, carbon, and molybdenum in solid-solution. Studies have found that in nickel-based chromium alloys, dislocation density interactions increase with temperature produces higher work hardening during plastic deformation [1-4]. Another study found that interaction between gamma prime and dislocations can accelerate plastic deformation formed due to tensile loading and lead to premature fracture at room temperature [5]. In contrast, another study found that tensile tests conducted at high temperatures tend to exhibit increased plasticity and therefore a higher tensile strength. The mechanism may be interaction of dislocations that leads to the initiation and generation of new dislocations. The resultant increase in dislocation density increases dislocation motion [6]. The amount of plastic deformation has been interpreted in terms of the development of dislocation structure and slip deformation.

A wide range of FCC alloys have been studied to investigate the effects of alloying elements on intergranular fracture, including the effect of Cr addition on tensile properties and fracture morphology of alloys with Ni, Cr, and Fe. The results show ductile brittle ductile transition during aging and enhanced tensile properties [7,8].

The contribution of this paper is an investigation of the effects of Cr and Mo additions on the tensile properties and grain boundary fracture behavior, as well as the appearance of slip bands and how these impact the plasticity of IN600 (Ni-16%Cr), IN601 (Ni-22%Cr) and C22 (Ni-22%Cr-14%Mo) alloys (wt %).

II. EXPERIMENTAL PROCEDURE

Since different batches of as-received materials may have different degrees of cold working as can be seen in Figure 2 (a), an annealing procedure was followed to ensure that the tensile properties of the three alloys would be free of the influence of different levels of cold working. Three annealing times for the as-received alloys – 1, 2 and 4 hours – at a temperature of 1000^{o}C were used to produce specimens for tensile testing. The three alloys were machined into tensile specimens as shown in Figure 1.

Figure 1. Photograph of tensile specimen with ductile fracture (a) before and (b) after tensile testing

III. RESULTS AND DISCUSSIONS

3.1 Stress strain curves (SSCs)

The following properties were obtained from the stress-strain curves: yield strength ($\sigma_{Y.S}$), ultimate tensile strength (σ_{UTS}), and fracture strength (σ_{FS}).

Examination of stress strain curves (Figure 2 and Table 1) shows that the tensile properties of the three alloys annealed for 1 hour were essentially identical to the properties of the alloys annealed at 1000C^o for 2 and 4 hours. In addition to tensile tests, Rockwell Hardness Tests were carried out to further characterize and confirm the tensile properties of these alloys. Average values for IN600, IN601, and C22 were 90, 92, and 90 HRB, respectively.

On the basis of these results, it was decided to use specimens annealed at 1000C^o for 1 hour to study morphology of intergranular fracture and slip bands.

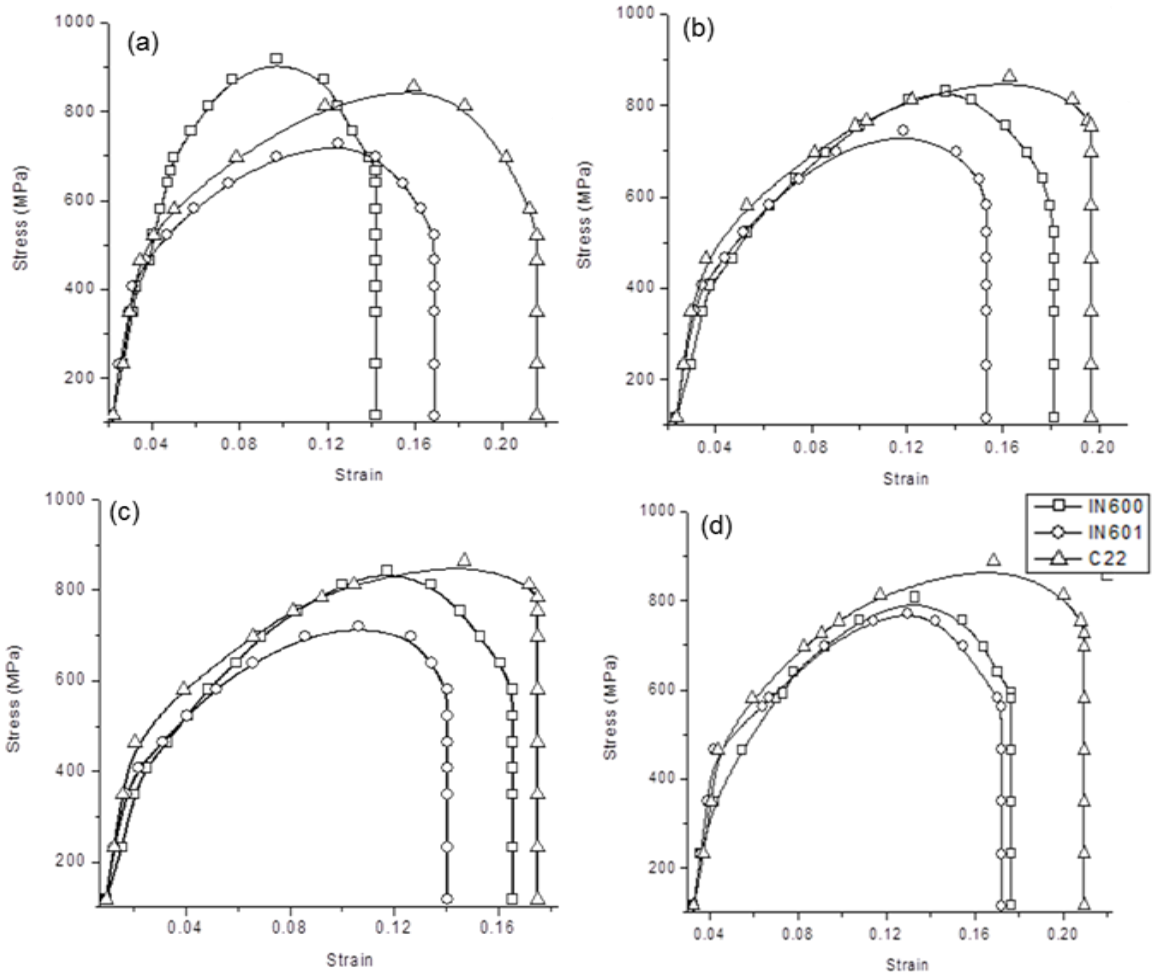

Figure 2. SSC's of (a) as-received and annealed at 1000C^o for (b) 1hr., (c) 2 hrs and (d) 4 hrs.

Table 1 Tensile properties (a) as received, and annealed at 1000C^o for (b) 1 hr., (c) 2 hrs and (d) 4 hrs.

(a) Alloy	σ_{YS} MPa	σ_{UTS} MPa	% Elongation
IN600	430	900	14
IN601	450	725	17
C22	450	850	22

(b) Alloy	σ_{YS} MPa	σ_{UTS} MPa	% Elongation
IN600	350	790	18
IN601	450	780	17
C22	450	850	22

(c) Alloy	σ_{YS} MPa	σ_{UTS} MPa	% Elongation
IN600	400	825	18
IN601	400	725	16
C22	450	850	20

(d) Alloy	σ_{YS} MPa	σ_{UTS} MPa	% Elongation
IN600	400	825	17
IN601	400	700	14
C22	450	850	18

SSCs as shown in Figure 2 (a) for as received IN600 exhibit higher strengths than IN601 and C22. In Figure 2 (b), IN600 and IN601 exhibit nearly identical elastic behavior and similar strain hardening response. However, C22, with Mo content, exhibits a higher σ_{UTS} and a higher plastic deformation. After the onset of necking, the specimens develop, especially C22 with its Mo content, additional larger plastic strains prior to final fracture as shown in Figure 3.

As shown in Table 1 (a) and Figure 2 (a), the SSC of IN600 exhibits a σ_{YS} of 430MPa, a σ_{UTS} of 900 MPa, and a σ_{FS} of approximately 700 MPa. In the same Figure, the SSC's of IN601 and C22 give values of σ_{YS} of 450MPa, and σ_{UTS} of IN601 approximately 725MPa. However, SSCs of C22 exhibited a σ_{UTS} of 850 MPa. Also, in the same Figure the SSC's of IN601 and C22 give values of σ_{FS} of approximately 500 MPa.

In comparing IN600, IN601 and C22 it may be observed that IN600 and IN601 exhibit only slightly different strengths and ductilities, whereas, C22 exhibits a significantly higher strength and ductility (Figure 2 (b)). This difference may be due to the addition of Mo in C22.

Table 1 (b) shows ductilities of IN600, IN601, and C22 of 18, 17, and 22, respectively. The ductility of C22 is greater than that of IN600 and IN601, neither of which have any Mo content in all of these conditions.

3.2 Microstructural Observations

Tensile fracture surfaces of these alloys were examined by scanning electron microscope (SEM) to evaluate the relationship between intrinsic microstructural features and the strength, ductility and intergranular fracture of each alloy.

Figures 3 (a), 3 (b), and 3 (c) show the fracture surfaces for IN600, IN601, and C22 specimens, respectively. In each case, a ductile dimpled intergranular fracture is indicated. C22 with Mo content (Figure 3(c)) shows more homogenous distribution of dimpling throughout the matrix and more precipitates observed along the grain boundary (Figure 6) than IN600 and IN601.

Further analysis was carried out using the computer program software (JMatPro). It was determined that gamma (γ) and $M_{23}C_6$ are the most common type of phase precipitates at the grain boundaries [9]. This is reasonable given that the grain boundaries act as sinks for precipitation and segregation (Figure 4) and provide a preferred location for intergranular fracture. This property is a consequence of the addition of Cr in IN600, IN601 and C22 and represents a major problem for these alloys due to segration of gmma precipitates at the grain boundaries.

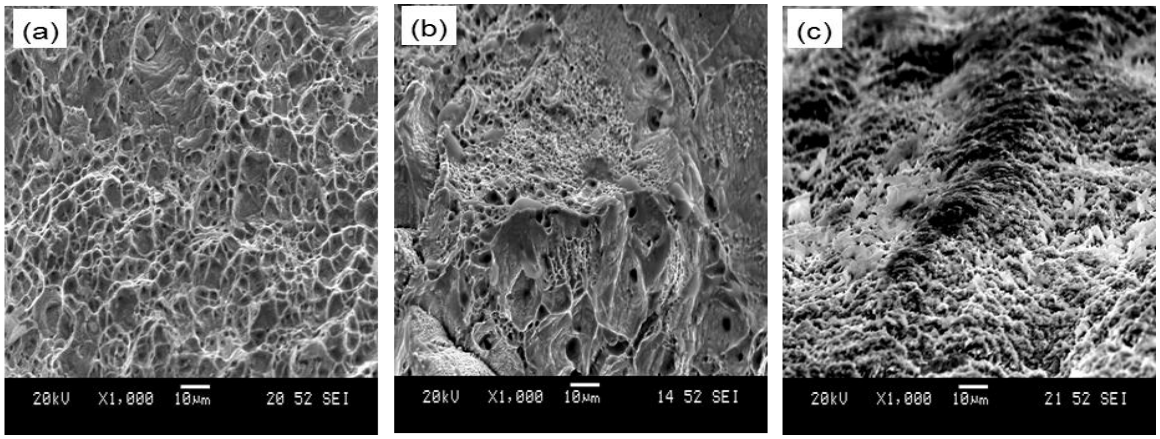

Figure 3. SEM micrographs indicating dimpled ductile fracture of (a) IN600, (b) IN601 and (c) C22.

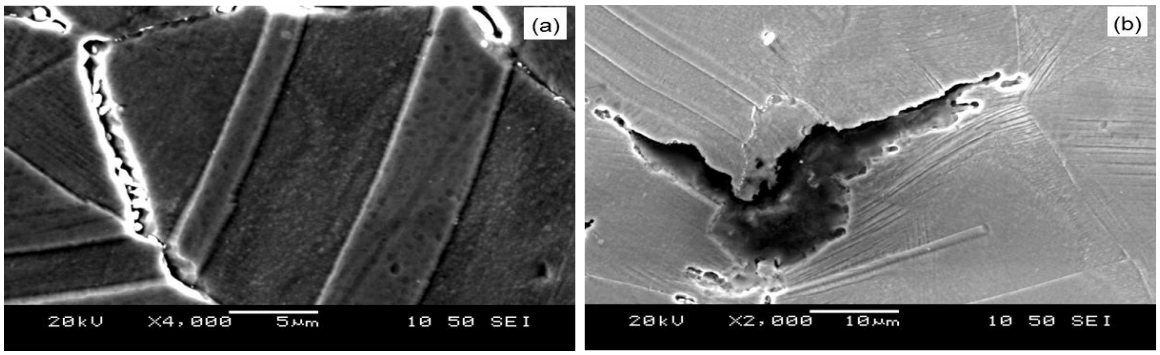

Figure 4. Precipitation and segregation of γ and $M_{23}C_6$ in grain boundaries leading to intergranular fracture in the three alloys.

Microstructural characterizations of slip bands were observed within an individual grain in any of each alloy. These slips effect the tensile properties and plastic deformation in the tensile test. Incompatible deformations of neighboring grains must be accommodated by elastic or plastic deformation in order to ensure the continuity of the deformed material [7].

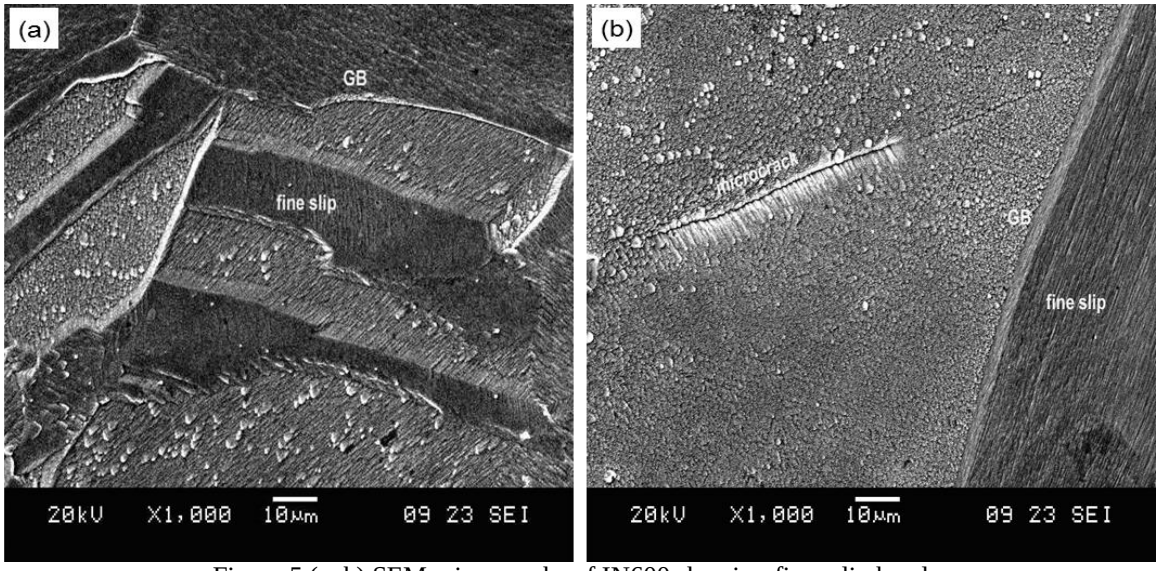

Figure 5 (a, b) SEM micrographs of IN600 showing finer slip bands.

Figure 5 shows IN600 with a very small amount of precipitates along the grain boundaries. The slip bands are fine and small (Figure 5 (a, b)).
Figure 6 shows IN601 with more precipitates along grain boundaries, more slip band arrays indicated within the grains, and different orientations in each grain.

.

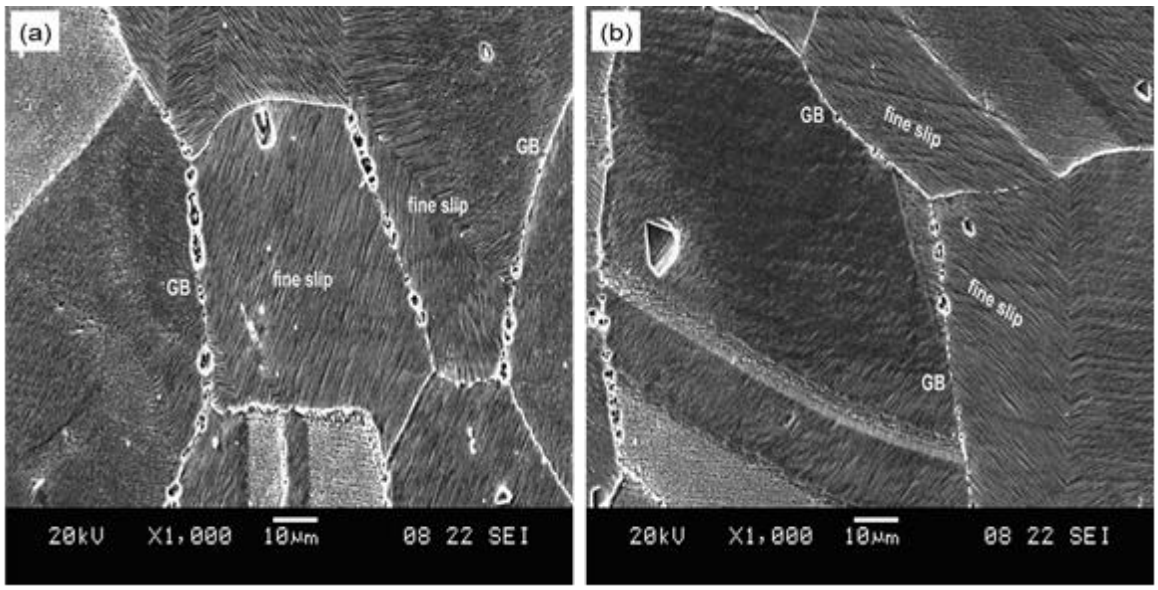

Figure 6 (a, b) SEM micrographs of IN601 showing precipitates along grain boundaries and slip bands within grains

Precipitates within grain boundaries create stress concentrations and lead to intergranular fracture. More obvious slip bands were observed within grains as shown in images in Figure 6 (a, b).
It should be noted that grain boundary micro cracks are responsible for an increased effective stress and accelerated tensile failure. Moreover, the large grain size accelerates crack growth as long as the crack propagates along the same grain boundary. However, the high density of slip bands prevents further propagation of crack growth. Therefore, the more slip bands generated during uniaxial tensile testing, the larger the amount of plastic deformation as well as the delaying of fracture, as shown in Figures 7 (a) and 7 (b).

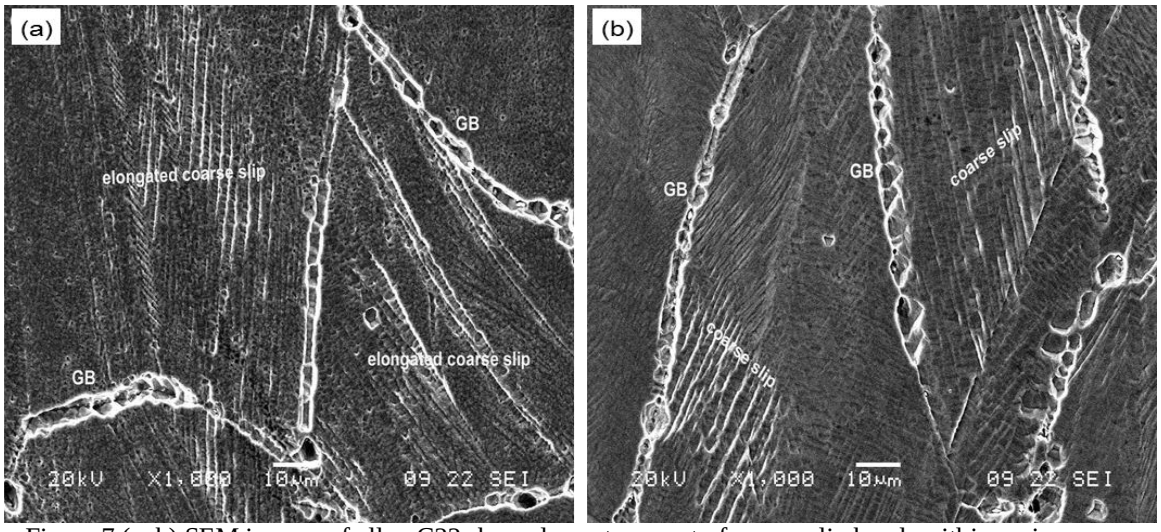

Figure 7 (a, b) SEM images of alloy C22 shows largest amount of coarse slip bands within grains.

It appears that the addition of more Cr and Mo results in locally scattered but large numbers of slip bands within grains. Consequently, the effect of Cr and Mo additions is significant, even in the elastic region as shown in Figures 3 (b), 3 (c) and 3 (d). Addition of Mo increases the σ_{YS} and σ_{UTS} and % elongation. Solid-solution hardening effects and the slip band substructure due to Mo are responsible for the strength enhancement in alloy C22.

IV. CONCLUSION

Uniaxial tensile test results indicate that C22 has higher tensile properties than IN601 and IN600. Fracture surfaces in all three alloys show ductile dimpled fracture but are finer and more numerous in C22 than in IN601 and IN600. Gamma (γ) and $M_{23}C_6$ precipitation were most pronounced along grain boundaries. These boundaries are proposed as the source of intergranular failure of these alloys. Additions of Cr and Mo enhanced grain boundary precipitation.

It was also been found from microstructural observations that higher amounts of slip bands occurred within grains of C22 than for IN601 and IN600 and account for the higher plastic deformation in C22 than in IN601 and IN600.

REFERENCES

[1] H. Akio. S. Kentaro, KF Koboyashi, Microstructure and mechanical properties of laser beam welded Inconel 718, *International Journal of Material Production Technology 13 (1-2),* 1998, 28-44.

[2] J. G. Gonzalez, Effect of structural evolution in IN601 on intergranular corrosion, *Material Chemistry. Physics 56 (1),* 1998, 70-73.

[3] X. Lin and X. Chen, Laser ablation rates of Inconel and aluminum with femo and nanosecond pulses, in *Proceedings of CLEO*. San Francisco 1998.

[4] V. Vankahtesh, and H. J. Rack, Elevated temperature hardening of IN690, *Journal of Mech. Material, 30 (1),* 1998, 69-81.

[5] M. C. Pandey, and D. V. V. Satyanarayana, Effect of gamma prime depletion on creep behavior of a nickel base superalloy, *Journal of Material Science, Vol. 19 (6),* 1996, 1009-1015.

[6] V. P. Swaminathan, H. B. Owens, and N. Hicks, Evaluation of gas turbine, *International Gas Turbine and Aerospace Congress and Exposition Conference,* Cologne, Germany, 1992.

[7] D. R. Squires, F. G. Wilson and E. A. Wilson, Modeling of precipitation kinetics and age hardening of Fe-Ni-Mn maraging type alloy, *Materials Science and Technology, Vol. 18,* 2002, 377-382.

[8] S. J. Kim, and C. M. Wayman, Effects of aging temperature on the microstructure and mechanical properties of 1.8Cu-7.3Ni-15.9Cr-1.2Mo-low C, N martensitic precipitation hardening stainless steel, *Material Science Engineering A. 35,* 2000, 2245-2253.

[9] A. Mohamed and T. Mohamed, Ni-based Cr alloys and grain boundaries characterization, *International Journal of Computational Engineering Research, Vol, 03(5),* 2013, 69-72.